35th Annual International Conference of the IEEE EMBS
Osaka, Japan, 3 - 7 July, 2013

Reduction of EEG artefacts induced by vibration in the MR-environment

Sven Rothlübbers[1] Vânia Relvas[1] Alberto Leal[2] Patrícia Figueiredo[1]

Abstract— **The EEG acquired simultaneously with functional magnetic resonance imaging (fMRI) is distorted by a number of artefacts related to the presence of strong magnetic fields. In order to allow for a useful interpretation of the EEG data, it is necessary to reduce these artefacts. For the two most prominent artefacts, associated with magnetic field gradient switching and the heart beat, reduction methods have been developed and applied successfully. Due to their repetitive nature, such artefacts can be reduced by subtraction of the respective template retrieved by averaging across cycles. In this paper, we investigate additional artefacts related to the MR environment and propose a method for the reduction of the vibration artefact caused by the cryo-cooler compression pumps system. Data were collected from the EEG cap placed on an MR head phantom, in order to characterise the MR environment related artefacts. Since the vibration artefact was found to be repetitive, a template subtraction method was developed for its reduction, and this was then adjusted to meet the specific requirements of patient data. The developed methodology successfully reduced the vibration artefact by about 90% in five EEG-fMRI datasets collected from two epilepsy patients.**

I. INTRODUCTION

Since the first reports almost two decades ago, the simultaneous acquisition of the electroencephalography (EEG) with functional magnetic resonance imaging (fMRI) has become an increasingly popular tool for the study of human brain function [1], [2]. One of the greatest challenges in EEG-fMRI experiments is the reduction of a number of different kinds of artefacts that deteriorate the EEG signal acquired inside the magnetic resonance (MR) environment. Unwanted induction on the EEG equipment connecting wires can be caused by magnetic field changes due to: gradient switching during fMRI acquisitions; patient movement or system vibration modifying the area of the conducting loops formed by the wires; or even more complex interactions between patient physiology and magnetic field, such as the ones leading to the pulse artefact [3]. Because these artefacts may be of the same order of magnitude or even several order of magnitude higher than the physiological EEG, their reduction is necessary for a meaningful examination of the EEG data.

Since inductive artefacts can be assumed to add to the EEG signal linearly, common methods to reduce them involve the subtraction of an artefact template from the measured signal. For repetitive artefacts, the template may be retrieved by averaging across cycles and the method is then termed average artefact subtraction (AAS). The gradient switching artefact occurs with the periodicity of the slice acquisition of the fMRI pulse sequence and it can be efficiently reduced using AAS [4]. The pulse artefact is also repetitive, but unlike the gradient switching artefact its period is unstable and its shape varies over time [5]. However, in this case the artefact in individual cycles can be estimated based on markers extracted from the electrocardiogram. With a AAS sliding window approach again it is possible to reduce the pulse artefact [6]. In general, artefact retrieval can also be supported by techniques such as principal component analysis [7] or independent component analysis [8].

Although the gradient and pulse artefacts are the most prominent ones to affect the EEG recorded simultaneously with fMRI, other artefacts have been shown to arise on the EEG signal as soon as this is recorded within the MR environment, even without ongoing fMRI acquisitions [9]. Indeed, external factors such as the cryo-cooler compression pumps, room lights and patient ventilation have been shown to produce visible artefacts on the EEG when switched on. The room lights and patient airflow can in principle always be turned off during the examination, avoiding the respective artefacts altogether. While it would be desirable to also turn off the cry-cooling system for EEG-fMRI studies, this is not allowed at some hospital sites and therefore vibration artefact reduction procedures may be required. The vibrations of the cooling pumps are transferred to the EEG equipment wires, causing induction inside the magnetic field and consequently pronounced oscillations on the EEG signals.

In this paper, we aim to investigate the artefacts that arise on the EEG signal when collected inside a 3 Tesla MR scanner and to develop a method to reduce the most relevant of such artefacts, due to vibrations induced by the cooling system. For this purpose, data will be collected from the EEG cap placed on an MR head phantom in order to characterise the MR environment related artefacts and particularly the vibration artefact. An AAS approach will then be taken in order to reduce the artefact from the EEG signal. The developed algorithm will then be applied to EEG-fMRI data collected from two epilepsy patients. A number of adjustments will be implemented to deal with additional requirements of the patient data, resulting in a modified final version of the artefact reduction method. In section II, the data collection and the proposed artefact reduction method are described. The results obtained are then presented in section III and a conclusion is finally given in section IV.

II. METHODS

A. Data Collection

Experimental data were acquired from a spherical MR head phantom as well as two epilepsy patients. The phantom

[1]Institute for Systems and Robotics / Instituto Superior Técnico, Technical University of Lisbon, Lisbon, Portugal

[2]Centro de Investigao e Intervenão Social / Department of Neurophysiology, Centro Hospitalar Psiquiátrico de Lisboa, Lisbon, Portugal

978-1-4577-0216-7/13/$26.00 ©2013 IEEE

data will be used to characterise the artefacts and develop a first iteration of the vibration artefact reduction method, while the patient data will be used to test and improve the method. In all measurements, EEG data were collected using a 32-channel EEG system (*Brain Amp* with *Brain Cap*, 56cm circumference, Brain Products, Gilching Germany) inside a 3 Tesla MR scanner (Siemens *Verio*, Erlangen Germany), at Hospital da Luz in Lisbon. The EEG cap was placed on the phantom or head within the head radio-frequency (RF) coil, and the amplifier and battery set was seated inside the bore of the scanner, and connected outside to the control room via a fibre-optic cable. The wires connecting the EEG cap to the amplifier were held straight along the scanner axis, and were supported with pillows along their path in some datasets in an attempt to minimize vibrations. Sandbags were also placed on top of the wires as well as the amplifier and battery set in order to minimize vibrations. The EEG data were collected using *Brain Vision Recorder* (Brain Products), with amplifier settings: high frequency cut-off of 250Hz; low frequency cut-off of 10s and sampling rate of 5000Hz.

In order to characterise MR environment related artefacts on the EEG signal recorded inside the scanner, the EEG cap was placed onto an MR head phantom (*Spherical Phantom D170*, 56cm circumference, Siemens) covered with a thin layer of EEG gel (*Abralyte 2000*, Brain Products). The patient's weight was simulated by a volunteer lying on the scanner bed. Different conditions hypothesized to affect the EEG artefacts were tested: room light on and off; patient ventilation on and off; EEG wires support on and off; and two different patient's weights. It was not possible to switch off the cooling pump due to internal hospital guidelines. Two minutes of EEG data were collected for seven combinations of these conditions, without MR scanning.

The EEG was acquired concurrently with fMRI scans using gradient-echo echo-planar-imaging, from two epilepsy patients. In Patient 1, 40min of EEG-fMRI data were collected and one 15s seizure was registered. In Patient 2, 30min of EEG-fMRI data were collected, with recurring inter-ictal spikes registered throughout. No preprocessing filters were applied to the EEG data and to allow for optimal correction the sampling rate was left unchanged. Before further processing, data were corrected for the gradient and pulse artefacts using *Brain Vision Analyzer* (Brain Products), with standard options and parameters.

B. Artefact Reduction

If the measured EEG signal $X(t)$ is given by a linear combination of the true, physiological EEG signal $X^*(t)$ and the superimposed artefacts $X_A(t)$, then an estimate of the true signal $\tilde{X^*}(t)$ can in principle be retrieved by subtracting an estimate of the artefact $\tilde{X_A}(t)$ from the measured signal:

$$\tilde{X^*}(t) = X(t) - \tilde{X_A}(t) \tag{1}$$

Since the artefact cannot be estimated perfectly, it cannot be completely removed but only reduced from the signal. Obtaining a good estimate of the artefact is therefore the main goal of the artefact reduction process and will be described over the next sub-sections.

1) Artefact Template: Retrieval of a periodic artefact can be achieved by segmenting the signal into the artefact's cycles and averaging across these. Consider the segmentation of the measured signal $X(t)$ into N adjacent segments with onsets S_i ($i = [0..N-1]$) and segment size $W_i = S_{i+1} - Si$. In case of a stable repetition period T, we have:

$$S_i = T \cdot i, \qquad W_i = T \quad \text{and} \quad X(S_i + t_d) = X(S_j + t_d) \tag{2}$$

for any delay t_d, such that $0 \leq t_d < T$. The artefact template can then be retrieved by computing the signal average across segments:

$$\tilde{X_A}(t_d) = \frac{1}{N} \sum_{i=1}^{N} X(S_i + t_d) \tag{3}$$

If the signal is not perfectly stable, then a sliding window approach should be employed, whereby only a limited number of neighboring segments, or windows, are used to recover the artefact of segment i:

$$\tilde{X_{Ai}}(t_d) = \frac{1}{2R+1} \sum_{j=-R}^{R} X(S_i + T \cdot j + t_d) \tag{4}$$

The number of windows $2R + 1$ determines the outcome of the removal. Averaging over a low number of segments may retrieve data with different periodicities than the desired one, while averaging over a high number may deteriorate the quality of the retrieval due to timing imprecision. In the present case, averaging over 21 windows provides a good balance provided the repetition period is matched.

If the repetition period is more unstable than what the sliding window approach can make up for, Eqs.2 are no longer valid and it will be necessary to compute the optimal local repetition period W_i for the whole time course before retrieving the artefact. The retrieval process is then obtained by a generalization of Eq.4 for segments of different sizes:

$$\tilde{X_{Ai}}(t_d) = \frac{1}{2R+1} \sum_{j=-R}^{R} X(S_i + W_i \cdot j + t_d) \tag{5}$$

2) Signal Segmentation: In order to achieve the signal segmentation into periods containing one repetition of the artefact, it is necessary to find the optimal repetition time of the artefact over time. Because the vibration artefact does not carry a distinguishing mark (comparable to the R-peak for the pulse artefact) nor are there any external markers available (comparable to the scanner triggers for the gradient artefact), in this case the computation of the optimal repetition period is performed based on the local signal auto-correlation (AC). The AC is computed for lags in the interval -15 to $+15$s around each time point, and the lag yielding the maximum AC value is selected as the optimal repetition period.

The process of signal segmentation therefore consists of the following steps: for the first time point S_1, a segment is added with size W_1 equal to the lag yielding the AC local maximum; the algorithm then advances to the end of the segment and another segment is added in a similar way for

the following time point S_2; the process is repeated until the whole signal is segmented in N segments. The artefact template is then obtained by signal averaging over adjacent segments of the same size as the segment being corrected.

Robustness of the segmentation against perturbations by physiological data and noise is assured in three ways. Firstly, the signal used for segmentation is the sum of the EEG across all channels, which improves the signal-to-noise ratio of the artefact estimate. This signal is then bandpass filtered to 95-105Hz, where the artefact is strongest compared to other signals. Finally, the AC maximum is only searched for lags in the range 0.996-1.004s, which is twice as large as the range of observed optimal repetition times, but still excludes many other AC local maxima.

3) Artefact Filtering: The previously described artefact template estimation algorithm can be used to retrieve the artefact, but it will also retrieve EEG data with the same periodicity but from other sources, particularly physiological. In order to remove falsely detected data from the artefact template, the previously retrieved artefact estimate over the whole time course is filtered in the frequency domain. Only artefact spectral peaks which stand out above the full signal spectrum are considered to belong to the artefact (Fig.1).

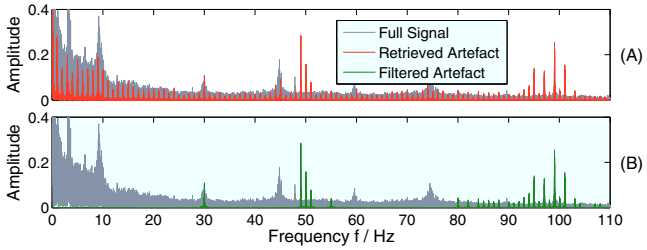

Fig. 1. Spectra of signal and artefact before (A) and after (B) filtering. The accepted peak at 30Hz is an example for a false positive, since it belongs to a residual of the gradient artefact correction and not the vibration artefact.

The exact frequencies of the artefact peaks (Fig.1 - red) are first determined by convolving the local spectrum around the frequencies $f_0(n) = n \cdot 1\text{Hz}, n = 1, 2, ...$ with a Lorentzian $L(f) = s^2/(s^2 - f^2)$ with width $s = 0.03$Hz and finding the frequency f that yields the maximum of this convolution. The spectrum of the full signal $S(f)$ is then locally weighted around each artefact peak (0.5Hz radius), once with the Lorentzian $A = \sum_f S(f)L(f)$ and once with its symmetric $B = \sum_f S(f)(1-L(f))$. If a peak satisfies $A > \xi B, \xi > 0$, it is kept in the artefact spectrum, otherwise it is set to zero, resulting in a filtered artefact (Fig.1 - green). The ξ value should be chosen semi-automatically so as to balance out the number of false positives and false negatives.

In order to stabilize and speed up the filtering process, peak detection is conducted on the EEG signal summed up across channels, yielding a binary frequency mask which is then used to filter the artefact estimates of each EEG channel. This results in the complete algorithm (Fig.2).

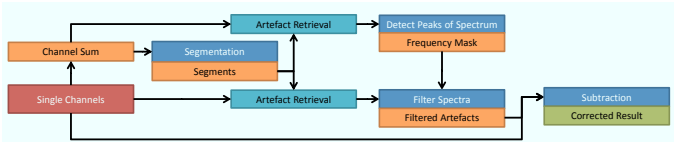

Fig. 2. Diagram illustrating the complete artefact reduction algorithm.

III. EXPERIMENTAL RESULTS

A. Artefact Characterisation

Three different types of artefacts can be distinguished on the EEG recorded from the phantom in the MR environment, as shown in Fig.3, which can also be identified on the patient data. One artefact is present in all datasets, occurring as a peak at 47.7Hz (Fig.3: B). This artefact is particularly visible on the phantom data and its source has yet to be determined. Artefacts associated with the patient ventilation system and the room lights can be identified as relatively smaller peaks between 97 and 99Hz (Fig.3: C).

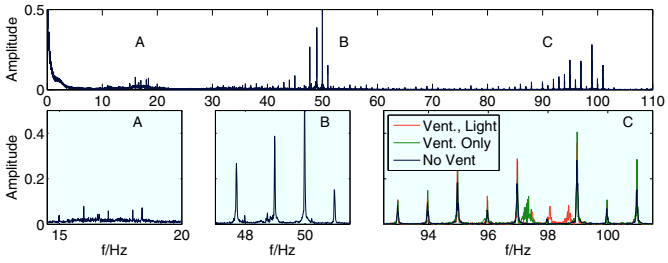

Fig. 3. Spectrum of the EEG signal recorded from the phantom in the MR environment, exhibiting the main artefacts in sections A, B and C.

The most prominent artefact presented as peaks around 50 and 100Hz, and extending into the whole spectrum, spaced by approximately 1Hz (0.998-1.002Hz) (Fig.3: A to C). It is attributed to the vibrations of the EEG-connecting wires induced by the cooling compression pump system. No significant changes in these artefacts were observed in relation to patient weight, while cable support affected the spacing of artefact peaks slightly. The artefact reduction algorithm was developed for this vibration artefact and the results of its application to real data are now presented.

B. Artefact Reduction

1) Signal Segmentation: The results of vibration artefact retrieval as a function of signal segmentation are shown in Fig.4 for one phantom dataset. It can be seen that the optimal artefact repetition period varies over time and that an adaptive segmentation based on the estimated optimal repetition periods is required in order to retrieve the artefact across the full time course. The optimal repetition periods were found to vary between datasets, but they were always within the range $[4990..5010]$ samples = $[0.998..1.002]$s.

2) Artefact Subtraction: Subtraction of the signal averaged across segments yielded complete removal of the artefact from the phantom data. However, such correction did not work satisfactorily on the patient data, due to the inclusion in the raw artefact template of EEG data from other sources. Filtration of the artefact was therefore required in order to obtain maximal artefact reduction. This is illustrated

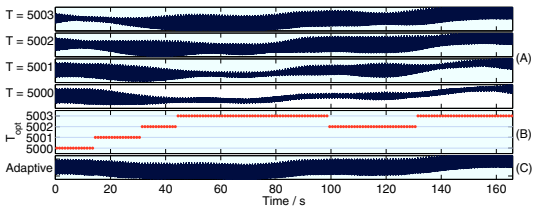

Fig. 4. Vibration artefact retrieval: with a fixed (A) and an adaptive (C) repetition period T (in samples), which uses the optimal repetition rate T_{opt} of the single segments (B) (Data: Head phantom, representative channel).

by the results obtained in a period of the EEG collected from Patient 1 where a seizure started (Fig.5). Time-frequency analysis obtained by Morlet wavelet decomposition clearly shows that filtering successfully kept only the true artefact components hence preventing removal of physiological data of interest from the EEG, particularly in the low frequencies. The algorithm was also able to efficiently reduce the artefact without removing information of interest from the EEG in Patient 2 (results not shown). Special attention was given to the seizure in Patient 1 and the interictal spikes in Patient 2, which could be fully recovered after artefact reduction.

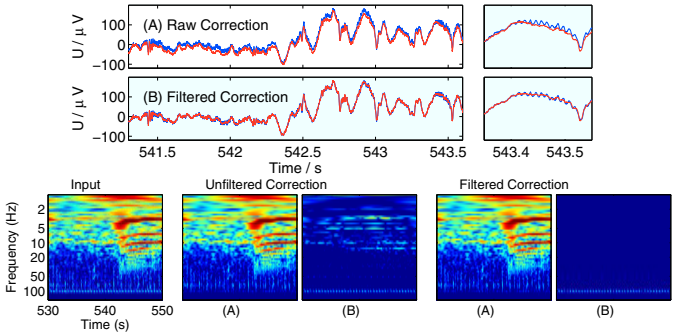

Fig. 5. Artefact reduction. Top) Uncorrected (blue) and corrected (red) signal, using the raw (A) and filtered (B) artefact template. Bottom) Time-frequency-analysis of: EEG signal before correction (left); EEG signal corrected (middle-A) by raw artefact template (middle-B) and EEG signal corrected (right-A) by filtered artefact template (right-B). (Data: Patient 1, Beginning of seizure, Channel CP2).

Overall, application of the proposed algorithm reduced the main artefact peaks at 50, 99 and 101Hz by $90 \pm 5\%$ in every EEG channel of every dataset. These values were obtained by comparing the spectra before and after correction, weighted with Lorentzians at the detected peaks.

IV. DISCUSSION AND CONCLUSION

In this work, three types of artefacts could be distinguished on the EEG recordings taken with a phantom inside the MR scanner without image acquisition, among which the most prominent was the vibration artefact induced by the compression pump cooling system. A method for the reduction of this artefact was developed and applied to the data collected from the phantom as well as from two epilepsy patients. The results demonstrate that the proposed method is able to efficiently reduce the vibration artefact, while preserving the physiological data of interest, namely the observed epileptiform activity.

A potential limitation of the proposed methodology are the possible interactions with other events with similar periodicity on the EEG. The repetition rates of the pulse artefact can get very close to the one of the vibration artefact (about 1Hz). However, a preliminary pulse artefact correction was not found to spoil the correction of the vibration artefact. On the other hand, if the fMRI is acquired using a repetition time near 1s, interferences with the scanning artefact correction may be prevented by performing segmentation beforehand.

Although the vibration artefact can in principle be avoided by switching off the cooling system during an EEG-fMRI experiment, this is not possible in all sites. On the other hand, although most studies to date have focused on EEG frequencies below 50Hz, there is currently great interest in the study of higher frequencies, notably the γ-band and the so-called High Frequency Oscillations, which can be as high as 500Hz [10][11]. In this case, the presence of the vibration artefact would preclude the correct analysis of the frequencies of interest. The method proposed here may therefore have great impact on the correction of EEG-fMRI performed with cooling system switched on.

ACKNOWLEDGMENTS

This work was supported by the Portuguese Science Foundation through Projects PTDC/SAU-ENB/112294/2009 and PEst-OE/EEI/LA0009/2011, and the International Association for the Exchange of Students for Technical Experience.

REFERENCES

[1] A. Salek-Haddadi, K.J. Friston, L. Lemieux, and D.R. Fish, "Studying spontaneous eeg activity with fmri," *Brain Research Reviews*, vol. 43, no. 1, pp. 110 – 133, 2003.

[2] P. Ritter and A. Villringer, "Simultaneous eegfmri," *Neuroscience ; Biobehavioral Reviews*, vol. 30, no. 6, pp. 823 – 838, 2006.

[3] H. Laufs, J. Daunizeau, D.W. Carmichael, and A. Kleinschmidt, "Recent advances in recording electrophysiological data simultaneously with magnetic resonance imaging," *NeuroImage*, vol. 40, pp. 515–528, 2008, PMID: 18201910.

[4] P.J. Allen, Giovanni Polizzi, Karsten Krakow, David R. Fish, and Louis Lemieux, "Identification of eeg events in the mr scanner: The problem of pulse artifact and a method for its subtraction," *NeuroImage*, vol. 8, no. 3, pp. 229 – 239, 1998.

[5] S. Debener, K.J. Mullinger, R.K. Niazy, and R.W. Bowtell, "Properties of the ballistocardiogram artefact as revealed by eeg recordings at 1.5, 3 and 7 t static magnetic field strength," *International Journal of Psychophysiology*, vol. 67, no. 3, pp. 189 – 199, 2008, ¡ce:title¿Integration of EEG and fMRI¡/ce:title¿.

[6] P.J. Allen, O. Josephs, and R. Turner, "A method for removing imaging artifact from continuous eeg recorded during functional mri," *NeuroImage*, vol. 12, no. 2, pp. 230 – 239, 2000.

[7] R.K. Niazy, C.F. Beckmann, G.D. Iannetti, J.M. Brady, and S.M. Smith, "Removal of fmri environment artifacts from eeg data using optimal basis sets," *NeuroImage*, vol. 28, no. 3, pp. 720 – 737, 2005.

[8] S. Debener, A. Strobel, B. Sorger, J. Peters, C. Kranczioch, A.K. Engel, and R. Goebel, "Improved quality of auditory event-related potentials recorded simultaneously with 3-t fmri: Removal of the ballistocardiogram artefact," *NeuroImage*, vol. 34, no. 2, pp. 587 – 597, 2007.

[9] K. Mullinger, M. Brookes, C. Stevenson, P. Morgan, and R. Bowtell, "Exploring the feasibility of simultaneous electroencephalography/functional magnetic resonance imaging at 7 t," *Magnetic Resonance Imaging*, vol. 26, no. 7, pp. 968 – 977, 2008.

[10] H. Laufs, "Endogenous brain oscillations and related networks detected by surface eeg-combined fmri," *Human Brain Mapping*, vol. 29, no. 7, pp. 762–769, 2008.

[11] J.G.R. Jefferys, L.M. de la Prida, F. Wendling, A. Bragin, M. Avoli, I. Timofeev, and F.H. Lopes da Silva, "Mechanisms of physiological and epileptic hfo generation," *Progress in Neurobiology*, vol. 98, no. 3, pp. 250 – 264, 2012.